Acoustic radiation force on a heated spherical particle in a fluid including scattering and microstreaming from a standing ultrasound wave

Bjørn G. Winckelmann* and Henrik Bruus[†]
Department of Physics, Technical University of Denmark,
DTU Physics Building 309, DK-2800 Kongens Lyngby, Denmark
(Dated: 29 June 2023)

Analytical expressions are derived for the time-averaged, quasi-steady, acoustic radiation force on a heated, spherical, elastic, solid microparticle suspended in a fluid and located in an axisymmetric incident acoustic wave. The heating is assumed to be spherically symmetric, and the effects of particle vibrations, sound scattering, and acoustic microstreaming are included in the calculations of the acoustic radiation force. It is found that changes in the speed of sound of the fluid due to temperature gradients can significantly change the force on the particle, particularly through perturbations to the microstreaming pattern surrounding the particle. For some fluid-solid combinations, the effects of particle heating even reverse the direction of the force on the particle for a temperature increase at the particle surface as small as 1 K.

I. INTRODUCTION

A particle suspended in a fluid perturbed by an acoustic wave experiences a time-averaged force, termed the acoustic radiation force F^{rad} . Theoretical studies of F^{rad} date back to King in 1934 [1] who assumed the particle to be incompressible and the surrounding fluid to be ideal, meaning zero viscosity and zero thermal conductivity. Subsequently, Yosioka and Kawasima [2] included the effects of particle compressibility in 1955, and the results were summarized and expressed on potential form by Gor'kov [3] in 1962. Doinikov published two series of papers taking into account the effects of fluid viscosity [4, 5] in 1994 and the effects of heat conduction [6-8]in 1997, where he included both the linear scattering of the acoustic wave and the nonlinear steady acoustic microstreaming developing around the particle. More recent developments were made by Settnes and Bruus in 2012 [9], Karlsen and Bruus in 2015 [10], and Doinikov, Fankhauser, and Dual in 2021 [11]. A detailed study of $\boldsymbol{F}^{\mathrm{rad}}$ on small particles in a thermoviscous fluid was conducted in our recent work [12]. Here, the effects of particle vibrations, acoustic scattering, temperature and density dependent material parameters, and thermoviscous microstreaming were included in the analytical derivation of $\boldsymbol{F}^{\mathrm{rad}}$, and it was found that microstreaming effects may dominate F^{rad} when the viscous- and thermal boundary layer widths δ_s and δ_t are comparable to or larger than the particle radius a. The importance of the microstreaming patterns for $F^{\rm rad}$, alongside recent studies of the acoustic body force due to temperature gradients by Joergensen and Bruus [13], motivated the present study of the acoustic radiation force on a heated spherical microparticle.

In this paper we derive analytical expressions for \mathbf{F}^{rad}

on a spherical elastic particle in a Newtonian fluid, including adiabatic acoustic scattering and microstreaming, based on an extension of the theoretical framework presented in Refs. [4–6, 12]. In this extension we include a quasi-steady background temperature field with gradients, which we calculate from a purely diffusive heat equation. The particle radius a is assumed to be much smaller than the wavelength λ of the incident acoustic wave. The acoustic field is assumed to be adiabatic, which is a good approximation in the limit of $5\delta_t \lesssim a \ll \lambda$ [12]. Previously, Lee and Wang in 1984 and 1988 [14, 15] studied the special case of a heated (or cooled) heavy rigid sphere in an ideal inviscid gas, and without taking acoustic microstreaming into account in their analysis. They only considered a short-ranged temperature field, but here we argue that the primary change of $\boldsymbol{F}^{\mathrm{rad}}$ is caused by heating of the bulk fluid surrounding the particle, and we therefore reach different conclusions than Lee and Wang.

Unlike previous studies of thermal and viscous contributions to $\boldsymbol{F}^{\rm rad}$ [4–10, 12], we find that effects of externally generated thermal gradients may alter $\boldsymbol{F}^{\rm rad}$ on particles in the long-wavelength limit even for small boundary layer widths $\delta \ll a$. This may lead to new possibilities for acoustic handling of above µm-sized particles at MHz ultrasound frequencies through the use of heat sources.

The paper is structured as follows: governing equations are presented in Section II, our mathematical model is presented and solved in Section III, the results for an incident, standing, plane wave are analyzed in Section IV, and finally we conclude in Section V. Some mathematical details are presented in Appendices A and B, and supporting MATLAB scripts, numerical simulations in Comsol Multiphysics, and details on material parameters are provided in the Supplemental Material [16].

II. GOVERNING EQUATIONS

Our model includes an isotropic, elastic, solid particle suspended in a Newtonian fluid. The particle is assumed

^{*} winckel@dtu.dk

[†] bruus@fysik.dtu.dk

to be heated by either an external source (e.g. a laser) or an internal source (e.g. an exothermic chemical reaction), and consequently heat conduction leads to the formation of a temperature gradient in the surrounding fluid. The fluid is perturbed by a monochromatic adiabatic acoustic wave with frequency f and angular frequency $\omega = 2\pi f$. All physical fields $g(\mathbf{r},t)$ describing the system in space \mathbf{r} and time t are expanded in perturbation series, and the material parameters $q(\mathbf{r},t)$ vary through their dependency of temperature T and density ρ ,

$$g(\mathbf{r},t) = g_0(\mathbf{r},t) + \operatorname{Re}\left[g_1(\mathbf{r},t) e^{-i\omega t}\right] + g_2(\mathbf{r},t),$$
 (1a)

$$q = q_0[T_0(\boldsymbol{r}, t)] + \operatorname{Re}\left[q_1(\boldsymbol{r}, t) e^{-i\omega t}\right],$$
 (1b)

$$q_{1}(\mathbf{r},t) = \left(\frac{\partial q}{\partial T}\right)_{T=T_{0}} T_{1}(\mathbf{r},t) + \left(\frac{\partial q}{\partial \rho}\right)_{\rho=\rho_{0}} \rho_{1}(\mathbf{r},t). \tag{1c}$$

The zeroth-order fields $g_0(\mathbf{r},t)$ describe a quiescent fluid, with a background temperature field $T_0(\mathbf{r},t)$, and the zeroth-order parameters $q_0(\mathbf{r},t)$ are assumed to be functions of T_0 only, so their density dependency is neglected in the following. The complex-valued first-order fields g_1 describe the linear acoustic response, which follows the actuation frequency f. The second-order fields $q_2(\mathbf{r},t)$ describe a non-linear response containing small secondorder harmonics and a steady time-averaged response. Only the time-averaged second-order effects are considered here, and they are denoted by angled brackets, e.g. $\langle g_2(\mathbf{r},t)\rangle$. The acoustic oscillations and streaming generally depend on the background temperature field $T_0(\mathbf{r},t)$ due to the temperature dependencies of all physical parameters q_0 . We assume that the temperature field develops on a timescale much slower than an acoustic oscillation period f^{-1} , and the complex-valued acoustic fields $q_1(\mathbf{r},t)$ are calculated as steady fields at any given time t using the instantaneous temperature field $T_0(\mathbf{r},t)$.

The objective is to compute $\mathbf{F}^{\mathrm{rad}}$ by the time average of the stress $\boldsymbol{\sigma}$ integrated over the vibrating particle surface $\partial\Omega(t)$ with normal vector \boldsymbol{n} ,

$$\mathbf{F}^{\mathrm{rad}} = \left\langle \oint_{\partial \Omega(t)} \mathbf{\sigma} \cdot \mathbf{n} \, \mathrm{d}S \right\rangle. \tag{2}$$

Assuming that the particle drift is negligible during an acoustic period, \mathbf{F}^{rad} can be written as [4, 10],

$$\mathbf{F}^{\mathrm{rad}} = \oint_{\partial\Omega_0} \langle \boldsymbol{\sigma}_2 - \rho_0 \boldsymbol{v}_1 \boldsymbol{v}_1 \rangle \cdot \boldsymbol{n} \, \mathrm{d}S, \tag{3}$$

where $\partial\Omega_0$ is the equilibrium surface of the particle, and \boldsymbol{v} is the velocity field of the fluid surrounding the particle.

A. Thermal diffusion

The temperature field is treated as a transient background field. Heat diffusion is assumed to dominate over the heat convection caused by the acoustic streaming $\langle v_2 \rangle$, thus we assume a low Péclet number,

$$P\acute{e} = \frac{L|\langle v_2 \rangle|}{D_0^{\rm th}} \ll 1, \qquad D_0^{\rm th} = \frac{k_0^{\rm th}}{\rho_0 c_{p0}}.$$
 (4)

Here, L is the characteristic length scale for heat diffusion, $|\langle \boldsymbol{v}_2 \rangle|$ is the magnitude of the steady streaming field in the fluid, D_0^{th} is the thermal diffusivity, ρ_0 is the mass density of the quiescent medium at a given temperature T_0 , k_0^{th} is the thermal conductivity, and c_{p0} is the specific heat capacity at constant pressure. The time average of the particle motion is assumed to be zero, and the temperature in both the solid particle and the fluid thus follow the heat diffusion equation,

$$\partial_t T_0 = \frac{1}{\rho_0 c_{p0}} \nabla \cdot \left(k_0^{\text{th}} \nabla T_0 \right) + \frac{1}{\rho_0 c_{p0}} P, \tag{5}$$

where P is the power density absorbed by the medium due to an external or internal source of energy.

We assume that gradients in the temperature field T_0 are small enough that material parameters q_0 only deviate slightly from their ambient value q_0^{∞} , and that the change is linear in the deviation ΔT_0 from the ambient temperature,

$$\Delta T_0(\mathbf{r}, t) = T_0(\mathbf{r}, t) - T_0^{\infty}$$
(6a)

$$q_0 \approx q_0^{\infty} (1 + a_q \Delta T_0), \qquad a_q = \frac{1}{q_0^{\infty}} \left(\frac{\partial q_0}{\partial T}\right)_{T_0^{\infty}}, \quad (6b)$$

$$|a_q \Delta T_0| \ll 1,\tag{6c}$$

and terms containing
$$\partial_r T_0(\mathbf{r}, t)$$
 are neglected. (6d)

The assumption (6d) is justified by a numerical study presented in the Supplemental Material [16]. The assumption is based on the fact that the temperature field ΔT_0 falls off as $\Delta T_0 \sim r^{-1}$, where r is the distance to the particle center, whereas $\partial_r T_0 \sim r^{-2}$. We argue that the primary perturbation to \mathbf{F}^{rad} is due to the enhancement of a directional microstreaming caused by temperature-induced, long-ranged perturbations of the acoustic fields in the bulk. Consequently, the dominating terms are likely to be the ones decaying slowly with r^{-1} .

B. Viscous fluid dynamics

The surrounding fluid is described by the fluid velocity field \boldsymbol{v} and the fluid stress tensor $\boldsymbol{\sigma}$ expressed in terms of the dynamic viscosity η , the bulk viscosity η^{b} , and the fluid pressure p.

$$\boldsymbol{\sigma} = \eta \left[\boldsymbol{\nabla} \boldsymbol{v} + (\boldsymbol{\nabla} \boldsymbol{v})^{\mathsf{T}} \right] + \left[(\eta^{\mathrm{b}} - \frac{2}{3}\eta)(\boldsymbol{\nabla} \cdot \boldsymbol{v}) - p \right] \mathbf{I}.$$
 (7)

The physical fields are governed by local conservation of mass and momentum. To derive the acoustic equations, we assume the adiabatic condition ds = 0 on the entropy

s per unit mass and apply an equation of state relating p and ρ ,

$$\partial_t \rho = \nabla \cdot (-\rho \mathbf{v}), \tag{8a}$$

$$\partial_t(\rho \mathbf{v}) = \mathbf{\nabla} \cdot (\boldsymbol{\sigma} - \rho \mathbf{v} \mathbf{v}),$$
 (8b)

$$ds = \frac{c_p}{T} dT - \frac{\alpha_p}{\rho} dp = 0, \tag{8c}$$

$$p = p(\rho). \tag{8d}$$

We also introduce the isentropic compressibility κ_s ,

$$\kappa_s = \frac{1}{\rho} \left(\frac{\partial \rho}{\partial p} \right)_s = \frac{1}{\rho c^2}, \quad \text{(fluids)},$$
(9)

where c is the speed of sound in the fluid.

The fluid fields and parameters are expanded as described by Eq. (1), and we assume that the initial state of the fluid is quiscent, $v_0 = 0$. With the assumption (6d), Eqs. (7) and (8) give the first-order acoustic response,

$$i\omega \frac{1}{c_0^2} p_1 = \rho_0 \nabla \cdot \boldsymbol{v}_1, \tag{10a}$$

$$-i\omega\rho_0 \boldsymbol{v}_1 = \eta_0 \nabla^2 \boldsymbol{v}_1 + \left(\eta_0^{\mathrm{b}} + \frac{1}{3}\eta_0\right) \boldsymbol{\nabla} (\boldsymbol{\nabla} \cdot \boldsymbol{v}_1) - \boldsymbol{\nabla} p_1.$$
(10b)

The adiabatic assumption in Eq. (8c) further dictates that the acoustic temperature field T_1 is proportional to the pressure p_1 ,

$$T_1 = \frac{\kappa_{s0}(\gamma_0 - 1)}{\alpha_{p0}} p_1, \quad \gamma_0 = 1 + \frac{\alpha_{p0}^2 T_0}{\rho_0 c_{p0} \kappa_{s0}}, \quad (11)$$

where we have introduced the usual ratio $\gamma_0 = c_{p0}/c_{v0}$ of the specific heat capacities. We then use $\rho_1 = c_0^{-2} p_1$ and combine Eqs. (1c) and (11),

$$\eta_1 = -B_c \frac{\nu_0}{c_0^2} p_1,\tag{12a}$$

$$\eta_1^{\rm b} = -B_{\rm c}^{\rm b} \frac{\nu_0}{c_0^2} p_1,$$
(12b)

$$B_{\rm c} = \left[\frac{1 - \gamma_0}{\alpha_{p0} \eta_0} \left(\frac{\partial \eta}{\partial T} \right)_{T_0} - \frac{\rho_0}{\eta_0} \left(\frac{\partial \eta}{\partial \rho} \right)_{\rho_0} \right], \tag{12c}$$

$$B_{\rm c}^{\rm b} = \left[\frac{1 - \gamma_0}{\alpha_{p0} \eta_0} \left(\frac{\partial \eta^{\rm b}}{\partial T} \right)_{T_0} - \frac{\rho_0}{\eta_0} \left(\frac{\partial \eta^{\rm b}}{\partial \rho} \right)_{\rho_0} \right]. \tag{12d}$$

The time-averaged second-order terms of Eqs. (7) and (8) describe the non-linear streaming response,

$$0 = \nabla \cdot \left\langle \rho_0 \boldsymbol{v}_2 + \frac{1}{c_0^2} p_1 \boldsymbol{v}_1 \right\rangle, \tag{13a}$$

$$\mathbf{0} = \nabla \cdot \langle \boldsymbol{\sigma}_2 - \rho_0 \boldsymbol{v}_1 \boldsymbol{v}_1 \rangle, \tag{13b}$$

$$ig\langle m{\sigma}_2 ig
angle = \eta_0 \Big[m{
abla} ig\langle m{v}_2 ig
angle + ig(m{
abla} ig\langle m{v}_2 ig
angle + ig(m{
abla} ig\langle m{v}_2 ig
angle \Big)^{\sf T} \Big] + ig(\eta_0^{
m b} - rac{2}{3} \eta_0 ig) ig(m{
abla} \cdot ig\langle m{v}_2 ig
angle ig) m{\mathsf{I}}$$

$$-\left\langle p_{2}\right\rangle \mathbf{I}+\left\langle \eta_{1}\left[\boldsymbol{\nabla}\boldsymbol{v}_{1}+\left(\boldsymbol{\nabla}\boldsymbol{v}_{1}\right)^{\mathsf{T}}\right]+\left(\eta_{1}^{\mathsf{b}}-\frac{2}{3}\eta_{1}\right)\left(\boldsymbol{\nabla}\cdot\boldsymbol{v}_{1}\right)\mathbf{I}\right\rangle. \tag{13c}$$

We note that the zeroth-order quantities c_0 , ρ_0 , η_0 , and $\eta_0^{\rm b}$ depend implicitly on the spatial coordinates \boldsymbol{r} through gradients in the background temperature $T_0(\boldsymbol{r},t)$.

C. Isotropic elastic solid mechanics

The linear elastic solid is described by the the mechanical displacement field u, and the solid stress tensor σ , which is expressed in terms of the transverse and longitudinal speeds of sound $c_{\rm tr}$ and $c_{\rm lo}$,

$$\boldsymbol{\sigma} = \rho c_{\text{tr}}^2 [\boldsymbol{\nabla} \boldsymbol{u} + (\boldsymbol{\nabla} \boldsymbol{u})^{\mathsf{T}}] + \rho (c_{\text{lo}}^2 - 2c_{\text{tr}}^2) (\boldsymbol{\nabla} \cdot \boldsymbol{u}) \mathbf{I}. \quad (14)$$

The mechanical displacement field u can then be determined in time and space from the Cauchy equation,

$$\rho \partial_t^2 \boldsymbol{u} = \boldsymbol{\nabla} \cdot \boldsymbol{\sigma}. \tag{15}$$

For solids, the isentropic compressibility κ_s can be expressed as,

$$\kappa_s = \frac{1}{\rho(c_{\text{lo}}^2 - \frac{4}{3}c_{\text{tr}}^2)}, \quad \text{(solids)}. \tag{16}$$

Expanding the fields into a perturbation series with $u_0 = 0$, one can describe the acoustic vibrations by,

$$-\rho_0 \omega^2 \boldsymbol{u}_1 = \rho_0 c_{\text{tr}0}^2 \nabla^2 \boldsymbol{u}_1 + \rho_0 \left(c_{\text{lo}0}^2 - c_{\text{tr}0}^2 \right) \boldsymbol{\nabla} (\boldsymbol{\nabla} \cdot \boldsymbol{u}_1), (17)$$

where we have used assumption (6d). Following Ref. [10], we also define the velocity field v_1 and the complex-valued "viscosity" η_0 of the solid by,

$$\mathbf{v}_1 = -\mathrm{i}\omega \mathbf{u}_1$$
 and $\eta_0 = \mathrm{i}\frac{\rho_0 c_{\mathrm{tr}0}^2}{\omega}$, for solids. (18)

The second-order response is not calculated for solids, as the time-averaged second-order velocity field is zero, and the steady thermal expansion is negligible.

III. MODEL

As illustrated in Fig. 1, the physical model consists of a spherical, heated, solid particle of radius a, which is centered at the origin of a spherical coordinate system (r, θ, φ) . The particle is surrounded by a viscous fluid of infinite extent, and an incident pressure wave with axisymmetry around the z-axis propagates in the fluid and scatters on the sphere. Since many of the same physical quantities are defined in both the solid and the fluid, we denote all fields and parameters in the solid at r < a with a prime, e.g. ρ'_0 and v'_1 , whereas the fluid fields and parameters at r > a remain unprimed, e.g. ρ_0 and v_1 . Ratios of parameters of the solid particle relative to the surrounding fluid are denoted by a tilde and the normalized radial coordinate by a hat,

$$\tilde{q}_0 = \frac{q_0'}{q_0}, \qquad \hat{r} = \frac{r}{a}.$$
 (19)

In the following derivation we largely use the same notation and basic partial-wave expansion as in our previous work [12].

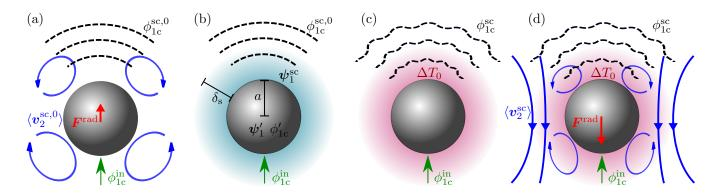


FIG. 1. (a) The standard constant-temperature case $\Delta T_0 = 0$ [4] of a spherical particle in an incident acoustic wave ϕ_{1c}^{in} (green arrow), which gives rise to the acoustic radiation force $\boldsymbol{F}^{\text{rad}}$ (red arrow) on the particle through scattered waves (such as $\phi_{1c}^{\text{sc},0}$, dashed lines) and microstreaming $\langle v_2^{\text{sc},0} \rangle$ (quadrupolar-like blue arrows). (b) Emphasizing further details of the standards case: the viscous scattering $\psi_1^{\rm sc}$ in the boundary layer (light blue) of width δ_s outside and the transmitted waves ϕ_{1c}' and ψ_1' inside the particle of radius a. (c) Heating of the particle gives rise to the temperature deviation ΔT_0 (light red) in the surrounding fluid. The scattered acoustic wave ϕ_{1c}^{sc} (warped dashed lines) for $\Delta T_0 > 0$ is significantly changed compared to $\phi_{1c}^{sc,0}$ in (a) and (b). (d) Acoustic scattering on the heated sphere with thermal contributions to both scattering and microstreaming $\langle v_2^{\rm sc} \rangle$ (blue), now with a significant directional component that leads to a modified acoustic radiation force $\boldsymbol{F}^{\mathrm{rad}}$ (red arrow).

The zeroth-order heat diffusion

When calculating the background temperature field, we assume that only the spherical solid particle is heated by the power source. Further, it is assumed that the power is uniformly absorbed throughout the particle, so the power density P is given by,

$$P(\mathbf{r},t) = P_0 \Theta(1-\hat{r})\Theta(t), \tag{20}$$

where $\Theta(\xi)$ is the Heaviside step function. sumptions (6) are applied to Eq. (5) neglecting terms $|a_q \Delta T_0| \ll 1$, and we solve for the temperature field T_0' inside the particle $(\hat{r} < 1)$, and T_0 outside $(\hat{r} > 1)$,

$$\partial_t T_0' = D_0^{\text{th}\infty'} \nabla^2 T_0' + \frac{1}{\rho_0^{\infty'} c_{p0}^{\infty'}} P_0, \quad t > 0,$$
 (21a)

$$\partial_t T_0 = D_0^{\text{th}\infty} \nabla^2 T_0. \tag{21b}$$

Initially for t < 0, the particle is assumed to be at ambient temperature T_0^{∞} . Then, at time t=0, the heating P is turned on. We apply continuity of temperature and heat flux, and the temperature is held at T_0^{∞} infinitely far from the sphere, so the boundary conditions are,

$$T_0(r,0) = T_0'(r,0) = T_0^{\infty},$$
 (22a)

$$T_0(a,t) = T_0'(a,t),$$
 (22b)

$$k_0^{\text{th}\infty} \partial_r T_0(a, t) = k_0^{\text{th}\infty'} \partial_r T_0'(a, t), \qquad (22c)$$

$$T_0(\infty, t) = T_0^{\infty}. \qquad (22d)$$

$$T_0(\infty, t) = T_0^{\infty}. (22d)$$

The heat diffusion problem in Eqs. (21) and (22) is treated in Ref. [17], where the solution is written as an integral to be numerically evaluated. However, as described in Appendix A, a good analytic approximation can be found for times $t\gtrsim 5t_{\rm d}^{\rm th},$ where $t_{\rm d}^{\rm th}$ is the characteristic timescale for heat diffusion over a particle radius. For polystyrene at room temperature we obtain,

$$t \gtrsim 5t_{\rm d}^{\rm th} = 5\frac{a^2}{D_0^{\rm th\infty}} \approx \left(\frac{a}{5\ \mu\rm m}\right)^2 \times 1\ \mathrm{ms}, \qquad (23)$$

which, for the particle sizes we consider here, is well below the timescale for the bulk fluid dynamics. In this longtime limit, the solution for the deviation $\Delta T_0(\hat{r},t)$ in the temperature of the fluid from the ambient T_0^{∞} becomes,

$$\Delta T_0(\hat{r},t) = \frac{\Delta T_0^{\rm surf}}{\hat{r}} \operatorname{erfc} \left[x_{\rm D}^{\rm th}(t) \, \hat{r} \right], \text{ for } t \gtrsim 5 t_{\rm d}^{\rm th}, \quad (24a)$$

$$x_{\rm D}^{\rm th}(t) = a \left(4D_0^{\rm th\infty}t\right)^{-\frac{1}{2}}, \quad \Delta T_0^{\rm surf} = \frac{P_0 a^2}{3k_0^{\rm th\infty}}, \quad (24b)$$

where ΔT_0^{surf} is the asymptotic value of the surface temperature of the particle. In the following theoretical derivation, $\Delta T_0(\hat{r},t)$ is the temperature profile (24).

В. The first-order acoustic scattering

The fluid is mechanically perturbed by an external, incident, acoustic wave that scatters on the particle. The first-order fluid fields are split into an incident (in) and a scattered (sc) field,

$$p_1 = p_1^{\text{in}} + p_1^{\text{sc}}, \qquad \boldsymbol{v}_1 = \boldsymbol{v}_1^{\text{in}} + \boldsymbol{v}_1^{\text{sc}}.$$
 (25)

Note that $p_1^{\rm in}$ and $\boldsymbol{v}_1^{\rm in}$ are the fields in the fluid at constantambient temperature $\Delta T_0 = 0$ and without the particle,

$$i\omega \frac{1}{c_0^{\infty 2}} p_1^{\text{in}} = \rho_0^{\infty} \nabla \cdot \boldsymbol{v}_1^{\text{in}}, \qquad (26a)$$

$$-\mathrm{i}\omega\rho_0^{\infty}\boldsymbol{v}_1^{\mathrm{in}} = -\boldsymbol{\nabla}p_1^{\mathrm{in}} + \eta_0^{\infty}\boldsymbol{\nabla}^2\boldsymbol{v}_1^{\mathrm{in}} + \left(\eta_0^{\mathrm{b\infty}} + \frac{1}{3}\eta_0^{\infty}\right)\boldsymbol{\nabla}(\boldsymbol{\nabla}\cdot\boldsymbol{v}_1^{\mathrm{in}}). \tag{26b}$$

The total fields p_1 and v_1 obey the governing equations in the heated fluid with $\Delta T_0 > 0$, and therefore the scattered fields $p_1^{\rm sc}$ and $v_1^{\rm sc}$ represent the presence of both the particle and of the temperature deviation in the fluid. Subtracting Eq. (26) from Eq. (10), we find the set of equations describing the scattered fields as,

$$\left(\frac{\mathrm{i}\omega}{c_0^2} - \frac{\mathrm{i}\omega}{c_0^{\infty 2}}\right) p_1^{\mathrm{in}} + \frac{\mathrm{i}\omega}{c_0^2} p_1^{\mathrm{sc}} = (\rho_0 - \rho_0^{\infty}) \nabla \cdot \boldsymbol{v}_1^{\mathrm{in}} + \rho_0 \nabla \cdot \boldsymbol{v}_1^{\mathrm{sc}},$$
(27a)

$$-i\omega(\rho_0 - \rho_0^{\infty})\boldsymbol{v}_1^{\text{in}} - i\omega\rho_0\boldsymbol{v}_1^{\text{sc}} =$$

$$(\eta_0 - \eta_0^{\infty})\nabla^2\boldsymbol{v}_1^{\text{in}} + \left[\left(\eta_0^{\text{b}} + \frac{1}{3}\eta_0\right) - \left(\eta_0^{\text{b}\infty} + \frac{1}{3}\eta_0^{\infty}\right)\right]\nabla(\nabla \cdot \boldsymbol{v}_1^{\text{in}})$$

$$+ \eta_0\nabla^2\boldsymbol{v}_1^{\text{sc}} + (\eta_0^{\text{b}} + \frac{1}{2}\eta_0)\nabla(\nabla \cdot \boldsymbol{v}_1^{\text{sc}}) - \nabla p_1^{\text{sc}}.$$
(27b)

We note that terms with prefactors $q_0 - q_0^{\infty}$ are explicitly caused by the gradient in T_0 , and thus do not appear in our previous work [12]. Consequently, in the following we encounter inhomogeneous Helmholtz equations, and we must re-derive the first-order solutions of Ref. [12].

As in Ref. [12], we solve the first-order acoustic scattering problem by Helmholtz decompositions of the velocities v_1^{in} (purely compressional) and v_1^{sc} of the fluid as well as v_1' of the particle,

$$\boldsymbol{v}_1^{\rm in} = \boldsymbol{\nabla} \phi_1^{\rm in}, \tag{28a}$$

$$\boldsymbol{v}_{1}^{\mathrm{sc}} = \boldsymbol{\nabla} \phi_{1}^{\mathrm{sc}} + \boldsymbol{\nabla} \times \boldsymbol{\psi}_{1}^{\mathrm{sc}}. \tag{28b}$$

$$\boldsymbol{v}_1' = \boldsymbol{\nabla} \phi_1' + \boldsymbol{\nabla} \times \boldsymbol{\psi}_1'. \tag{28c}$$

In Ref. [12], we split the scalar potentials ϕ_1 and ϕ'_1 into a compressional long-range part describing the weakly damped bulk waves and a thermal part describing the short-range thermal boundary layer. The thermal boundary layer drops out due to the adiabaticity assumption (8c), so ϕ_1 only refers to the compressional part. Inserting Eq. (28a) in Eq. (26), Eq. (28b) in Eq. (27), and Eqs. (28c) and (18) in Eq. (17), we derive that

$$\nabla^2 \phi_1' + k_c^{\prime 2} \phi_1' = 0, \quad k_c' = \frac{\omega}{c_{\text{loo}}'},$$
 (29a)

$$\nabla^2 \psi_1' + k_s'^2 \psi_1' = 0, \quad k_s' = \frac{\omega}{c_{tr0}'}, \tag{29b}$$

$$\nabla^2 \psi_1^{\rm sc} + k_{\rm s}^2 \psi_1^{\rm sc} = 0, \ k_{\rm s} = \frac{1+\mathrm{i}}{\delta_{\rm s}}, \ \delta_s = \left(\frac{2\eta_0^{\infty}}{\rho_0^{\infty}\omega}\right)^{\frac{1}{2}}, \ (29c)$$

$$\nabla^2 \phi_1^{\text{in}} + k_0^2 \phi_1^{\text{in}} = 0, \quad k_0 = \frac{\omega}{c_0^{\infty}},$$
 (29d)

$$\nabla^2 p_1^{\text{sc}} + k_0^2 p_1^{\text{sc}} = k_0^2 2a_c \Delta T_0 p_1^{\text{in}}, \tag{29e}$$

$$\boldsymbol{v}_{1}^{\mathrm{in}} = \frac{1}{\mathrm{i}\omega\rho_{0}^{\infty}} \boldsymbol{\nabla} p_{1}^{\mathrm{in}}, \qquad p_{1}^{\mathrm{in}} = \mathrm{i}\omega\rho_{0}^{\infty} \phi_{1}^{\mathrm{in}},$$
 (29f)

$$\boldsymbol{v}_{1}^{\mathrm{sc}} = \frac{1}{\mathrm{i}\omega\rho_{0}^{\infty}} \boldsymbol{\nabla} p_{1}^{\mathrm{sc}} - \frac{a_{\rho}\Delta T_{0}}{\mathrm{i}\omega\rho_{0}^{\infty}} \boldsymbol{\nabla} p_{1}^{\mathrm{in}} + \boldsymbol{\nabla} \times \boldsymbol{\psi}_{1}^{\mathrm{sc}}, \quad (29\mathrm{g})$$

$$a_c = \frac{1}{c_0^{\infty}} \left(\frac{\partial c_0}{\partial T} \right)_{T_0^{\infty}}, \quad a_{\rho} = \frac{1}{\rho_0^{\infty}} \left(\frac{\partial \rho_0}{\partial T} \right)_{T_0^{\infty}}.$$
 (29h)

Here, we have introduced the undamped compressional wave numbers k_0 and $k_{\rm c}'$, the shear wave numbers $k_{\rm s}$ and $k_{\rm s}'$, and the viscous boundary-layer thickness δ_s . Only the real part k_0 is taken into account in the wave number of the compressional wave in the fluid, as the imaginary part associated with damping is smaller by a factor $\Gamma_c = (\eta_0^{\rm bo} + \frac{4}{3}\eta_0^{\infty})\omega\kappa_{s0}^{\infty} \ll 1$. We have also neglected factors $|a_q\Delta T_0|\ll 1$ in the results of Eq. (29), except that terms of the form $a_q\Delta T_0p_1^{\rm in}$ are kept because $|p_1^{\rm in}|\gg |p_1^{\rm sc}|$. For our analysis, we introduce the normalized wave numbers,

$$x_0 = k_0 a, \quad x_s = k_s a, \quad x'_c = k'_c a, \quad x'_s = k'_s a, \quad (30)$$

and we note that we will be working in the longwavelength limit characterized by the small parameter,

$$x_0 \ll 1. \tag{31}$$

Eqs. (29a), (29b), (29c) and (29d) are all homogeneous Helmholtz equations with axisymmetric solutions expressed in terms of spherical Bessel functions $j_n(x)$, spherical outgoing Hankel functions $h_n^{(+)}(x)$ (called $h_n(x)$ in Ref. [12]), and Legendre polynomials $P_n(\cos \theta)$,

$$\phi_1^{\text{in}} = \sum_{n=0}^{\infty} A_n j_n(x_0 \hat{r}) P_n(\cos \theta),$$
 (32a)

$$\phi_1' = \sum_{n=0}^{\infty} A_n \alpha_{c,n}' j_n(x_c' \hat{r}) P_n(\cos \theta), \tag{32b}$$

$$\psi_1' = \mathbf{e}_{\varphi} \sum_{n=1}^{\infty} A_n \alpha_{s,n}' j_n(x_s' \hat{r}) \partial_{\theta} P_n(\cos \theta), \qquad (32c)$$

$$\psi_1^{\text{sc}} = \boldsymbol{e}_{\varphi} \sum_{n=1}^{\infty} A_n \alpha_{\text{s},n}^{\text{sc}} h_n^{(+)}(x_{\text{s}} \hat{r}) \partial_{\theta} P_n(\cos \theta).$$
 (32d)

The inhomogenous Helmholtz equation (29e) is solved by a partial-wave expansion for $p_1^{\rm sc}$,

$$p_1^{\text{sc}} = \sum_{n=0}^{\infty} p_{1,n}^{\text{sc}}(\hat{r}) P_n(\cos \theta),$$
 (33a)

$$\hat{\mathcal{D}}_{\hat{r}} p_{1,n}^{\text{sc}}(\hat{r}) = i \rho_0^{\infty} \omega \, 2a_c \Delta T_0 x_0^2 \hat{r}^2 j_n(x_0 \hat{r}), \tag{33b}$$

$$\hat{\mathcal{D}}_{\hat{r}} = \left[\frac{\mathrm{d}}{\mathrm{d}\hat{r}} \left(\hat{r}^2 \frac{\mathrm{d}}{\mathrm{d}\hat{r}} \right) - n(n+1) + x_0^2 \hat{r}^2 \right]. \tag{33c}$$

To construct a Green's function $G_n(\hat{r}, \xi)$ for Eq. (33b) that solves $\hat{\mathcal{D}}_{\hat{r}}G_n(\hat{r}, \xi) = \delta(\hat{r} - \xi)$, we introduce the incoming spherical Hankel functions $h_n^{(-)}(x)$. The Green's function $G_n(\hat{r}, \xi)$, which obeys the conditions of continuity, $G_n(\hat{r} = \xi^+, \xi) = G_n(\hat{r} = \xi^-, \xi)$, and the derivative jump, $\partial_{\hat{r}}G_n(\hat{r} = \xi^+, \xi) - \partial_{\hat{r}}G_n(\hat{r} = \xi^-, \xi) = \xi^{-2}$, is,

$$G_{n}(\hat{r},\xi) = \left\{ \left[B_{n}(\xi) + \frac{x_{0}}{2i} h_{n}^{(-)}(x_{0}\xi) \right] h_{n}^{(+)}(x_{0}\hat{r}) + C_{n}(\xi) h_{n}^{(-)}(x_{0}\hat{r}) \right\} \Theta(\hat{r} - \xi) + \left\{ \left[C_{n}(\xi) + \frac{x_{0}}{2i} h_{n}^{(+)}(x_{0}\xi) \right] h_{n}^{(-)}(x_{0}\hat{r}) + B_{n}(\xi) h_{n}^{(+)}(x_{0}\hat{r}) \right\} \Theta(\xi - \hat{r}).$$
(34)

Here, $B_n(\xi)$ and $C_n(\xi)$ are found from the remaining boundary conditions. Then, with $G_n(\hat{r}, \xi)$ given by Eq. (34), the solution to Eq. (33b) that satisfies the Sommerfeld radiation condition for outgoing waves, $\lim_{\hat{r}\to\infty} \left[\hat{r}\partial_{\hat{r}}\phi_{1,n}^{\rm sc}(\hat{r}) - \mathrm{i}x_0\hat{r}\phi_{1,n}^{\rm sc}(\hat{r})\right] = 0$, can be written as,

$$\begin{split} p_{1,n}^{\text{sc}}(\hat{r}) &= \mathrm{i} \rho_0^\infty \omega A_n \Big[\Big(\alpha_{\mathrm{c},n}^{\text{sc}} + I_n^{(-)}(\hat{r},t) \Big) h_n^{(+)}(x_0 \hat{r}) \\ &+ \Big(I_n^{(+)}(\infty,t) - I_n^{(+)}(\hat{r},t) \Big) h_n^{(-)}(x_0 \hat{r}) \Big], \ (35\mathrm{a}) \\ I_n^{(\pm)}(\hat{r},t) &= \frac{a_c x_0^3}{\mathrm{i}} \int_1^{\hat{r}} \xi^2 \Delta T_0(\xi,t) h_n^{(\pm)}(x_0 \xi) j_n(x_0 \xi) \, \mathrm{d}\xi. \end{split}$$

 $p_1^{\rm sc}$ from Eqs. (33a) and (35) reduces to the standard result when setting $\Delta T_0=0$, for which $I_n^{(\pm)}(\hat{r},t)=0$ and $\alpha_{\rm c,n}^{\rm sc}=\alpha_{\rm c,n}^{\rm sc,0}$. However, even for small temperature deviations ΔT_0 in the fluid, $p_1^{\rm sc}$ is significantly perturbed by thermal effects in a large region set by the thermal diffusion length, see details in the Supplemental Material [16]. Last, the constants $\left\{\alpha_{\rm c,n}^{\rm sc},\alpha_{\rm s,n}^{\rm sc},\alpha_{\rm c,n}',\alpha_{\rm s,n}'\right\}$ are found from the boundary conditions at the particle-fluid boundary, $\hat{r}=1$. The boundary conditions at the particle boundary are continuous velocity and stress,

$$v_{1r} = v'_{1r}, v_{1\theta} = v'_{1\theta}, (36a)$$

$$\sigma_{1\theta r} = \sigma'_{1\theta r}, \qquad \qquad \sigma_{1rr} = \sigma'_{1rr}.$$
 (36b)

In contrast to the six boundary conditions used in our work [12], we only need four here, because the adiabatic assumption excludes the thermal scalar potential and the corresponding two thermal scattering coefficients $\alpha_{t,n}^{\text{sc}}$, $\alpha_{t,n}'$ from the theory. Using the velocity potentials Eqs. (28) and (32), the stress tensors from Eqs. (7) and (14) with the pressures from Eqs. (29f), (33a) and (35), as well as the definition (18) of velocity and viscosity in the solid, we write the boundary conditions (36) expressed for each value of n as follows:

In (50) expressed for each value of
$$n$$
 as follows.
$$\frac{v_{1r} = v'_{1r}}{\alpha_{c,n}^{sc} x_0 h_n^{(+)'}(x_0) - \alpha_{s,n}^{sc} n(n+1) h_n^{(+)}(x_s)} - \alpha'_{c,n} x'_c j'_n(x'_c) + \alpha'_{s,n} n(n+1) j_n(x'_s)$$

$$= -x_0 j'_n(x_0) - I_n^{(+)}(\infty, t) x_0 h_n^{(-)'}(x_0), \qquad (37a)$$

$$\frac{v_{1\theta} = v'_{1\theta}}{\alpha_{c,n}^{sc} h_n^{(+)}(x_0) - \alpha_{s,n}^{sc} \left[x_s h_n^{(+)'}(x_s) + h_n^{(+)}(x_s) \right]} - \alpha'_{c,n} j_n(x'_c) + \alpha'_{s,n} \left[x'_s j'_n(x'_s) + j_n(x'_s) \right]$$

$$= -j_n(x_0) - I_n^{(+)}(\infty, t) h_n^{(-)}(x_0), \qquad (37b)$$

$$\frac{\sigma_{1\theta r} = \sigma'_{1\theta r}}{\alpha_{c,n}^{sc} 2\eta_0 \left[x_0 h_n^{(+)'}(x_0) - h_n^{(+)}(x_0) \right]} - \alpha_{s,n}^{sc} \eta_0 \left[x_s^2 h_n^{(+)''}(x_s) + (n^2 + n - 2) h_n^{(+)}(x_s) \right] - \alpha'_{c,n} 2\eta'_0 \left[x'_c j'_n(x'_c) - j_n(x'_c) \right] + \alpha'_{s,n} \eta'_0 \left[x'_s^2 j''_n(x'_s) + (n^2 + n - 2) j_n(x'_s) \right]$$

$$= -2\eta_0 \left[x_0 j'_n(x_0) - j_n(x_0) \right] - I_n^{(+)}(\infty, t) 2\eta_0 \left[x_0 h_n^{(-)'}(x_0) - h_n^{(-)}(x_0) \right], \qquad (37c)$$

$$\frac{\sigma_{1rr} = \sigma'_{1rr}}{\alpha_{c,n}^{sc} \eta_0 \left[(2x_0^2 - x_s^2) h_n^{(+)}(x_0) + 2x_0^2 h_n^{(+)''}(x_0) \right]}
- \alpha_{s,n}^{sc} \eta_0 2n(n+1) \left[x_s h_n^{(+)'}(x_s) - h_n^{(+)}(x_s) \right]
- \alpha'_{c,n} \eta'_0 \left[(2x_c^{'2} - x_s^{'2}) j_n(x_c^{'}) + 2x_c^{'2} j_n''(x_c^{'}) \right]
+ \alpha'_{s,n} \eta'_0 2n(n+1) \left[x_s^{'} j_n^{'}(x_s^{'}) - j_n(x_s^{'}) \right]
= -I_n^{(+)} (\infty, t) \eta_0 \left[(2x_0^2 - x_s^2) h_n^{(-)}(x_0) + 2x_0^2 h_n^{(-)''}(x_0) \right]
- \eta_0 \left[(2x_0^2 - x_s^2) j_n(x_0) + 2x_0^2 j_n''(x_0) \right].$$
(37d)

Note that for n=0, Eqs. (37b) and (37c) are void, so in this case only two equations with two unknown coefficients need to be solved. Similar to the corresponding boundary condition equations (52) in Ref. [12], we write Eq. (37) as a 4-by-4 matrix equation and apply Cramer's rule to find the scattering coefficients by expanding the involved determinants to leading order in x_0 . We use the following scalings in our derivation,

$$\Gamma_{\rm s}, I_n^{(\pm)}(\infty, t), \tilde{\eta}_0^{-1} \sim x_0^2, \qquad x_{\rm c}', x_{\rm s}', |a_q \Delta T_0| \sim x_0.$$
 (38)

For solid particles, only the two scattering coefficients $\alpha_{c,n}^{\text{sc}}$ and $\alpha_{s,n}^{\text{sc}}$ of the fluid are needed to calculate $\boldsymbol{F}^{\text{rad}}$. To leading order in x_0 , the coefficient $\alpha_{s,n}^{\text{sc}}$ is unchanged compared to the case $\Delta T_0 = 0$, whereas $\alpha_{c,n}^{\text{sc}}$ is,

$$\alpha_{\mathrm{c},n}^{\mathrm{sc}} = \alpha_{\mathrm{c},n}^{\mathrm{sc},0} + I_n^{(+)}(\infty, t), \tag{39}$$

where $\alpha_{\mathrm{c},n}^{\mathrm{sc},0}$ is the scattering coefficient evaluated at $\Delta T_0 = 0$. The expressions for $\alpha_{\mathrm{s},n}^{\mathrm{sc}}$ and $\alpha_{\mathrm{c},n}^{\mathrm{sc},0}$ to leading order in x_0 for n = 0, 1, 2, which are the coefficients needed to calculate $\boldsymbol{F}^{\mathrm{rad}}$, are found to be,

$$\alpha_{c,0}^{\text{sc},0} = -\frac{\mathrm{i}x_0^3}{3} [1 - \tilde{\kappa}_{s0}^{\infty}],$$
(40a)

$$\alpha_{c,1}^{\text{sc},0} = \frac{\mathrm{i} x_0^3}{3} \frac{(\tilde{\rho}_0^{\infty} - 1)[3(\mathrm{i} x_{\mathrm{s}} - 1) + x_{\mathrm{s}}^2]}{(2\tilde{\rho}_0^{\infty} + 1)x_{\mathrm{s}}^2 - 9(1 - \mathrm{i} x_{\mathrm{s}})},\tag{40b}$$

$$\alpha_{s,1}^{\text{sc}} = \frac{ix_0(\tilde{\rho}_0^{\infty} - 1)x_s^2 e^{-ix_s}}{(2\tilde{\rho}_0^{\infty} + 1)x_s^2 - 9(1 - ix_s)},$$
(40c)

$$\alpha_{c,2}^{\text{sc},0} = \frac{2ix_0^5}{15} \frac{6ix_s^2 + x_s^3 - 15(i + x_s)}{9x_s^2(i + x_s)},$$
(40d)

$$\alpha_{s,2}^{\rm sc} = -\frac{x_0^2 x_{\rm s} e^{-ix_{\rm s}}}{9(i+x_{\rm s})}.$$
 (40e)

C. The second-order steady streaming and F^{rad}

We now depart from assuming an arbitrary incident axisymmetric pressure wave and focus on the important special case of a standing plane wave. The incident pressure $p_1^{\rm in}(z)$ varies spatially along the z-axis with wave number k_0 , amplitude p_a , and phase shift k_0d ,

$$p_1^{\text{in}}(z) = p_a \cos[k_0(z+d)],$$
 (41)

which by comparing to Eqs. (29f) and (32a), corresponds to defining the incident wave by,

$$A_n = \frac{p_a}{i\rho_0^{\infty} \omega} \frac{2n+1}{2} i^n \left[e^{ik_0 d} + (-1)^n e^{-ik_0 d} \right].$$
 (42)

To evaluate $\mathbf{F}^{\mathrm{rad}}$, we compute the second-order timeaveraged fields, velocity $\langle \mathbf{v}_2 \rangle$ and pressure $\langle p_2 \rangle$. They are split into an incident (in) and a scattered (sc) part, where the former is assumed to be generated solely by the incident pressure field without any gradients in T_0 and with no suspended particle in the fluid,

$$\langle p_2 \rangle = \langle p_2^{\text{in}} \rangle + \langle p_2^{\text{sc}} \rangle,$$
 (43a)

$$\langle \boldsymbol{v}_2 \rangle = \langle \boldsymbol{v}_2^{\text{in}} \rangle + \langle \boldsymbol{v}_2^{\text{sc}} \rangle,$$
 (43b)

$$0 = \boldsymbol{\nabla} \cdot \left\langle \rho_0^{\infty} \boldsymbol{v}_2^{\text{in}} \right\rangle + \frac{1}{c_0^{\infty 2}} \boldsymbol{\nabla} \cdot \left\langle p_1^{\text{in}} \boldsymbol{v}_1^{\text{in}} \right\rangle, \tag{43c}$$

$$0 = \nabla \cdot \left\langle \eta_0^{\infty} \left[\nabla \boldsymbol{v}_2^{\text{in}} + \left(\nabla \boldsymbol{v}_2^{\text{in}} \right)^{\mathsf{T}} \right] + \left(\eta_0^{\text{bo}} - \frac{2}{3} \eta_0^{\infty} \right) \left(\nabla \cdot \boldsymbol{v}_2^{\text{in}} \right) \mathbf{I} - p_2^{\text{in}} \mathbf{I} + \eta_1^{\text{in}} \left[\nabla \boldsymbol{v}_1^{\text{in}} + \left(\nabla \boldsymbol{v}_1^{\text{in}} \right)^{\mathsf{T}} \right] + \left(\eta_1^{\text{b,in}} - \frac{2}{3} \eta_1^{\text{in}} \right) \left(\nabla \cdot \boldsymbol{v}_1^{\text{in}} \right) \mathbf{I} - \rho_0^{\infty} \boldsymbol{v}_1^{\text{in}} \boldsymbol{v}_1^{\text{in}} \right\rangle.$$
(43d)

Subtracting Eqs. (43c) and (43d) from Eq. (13), and using that $\langle \boldsymbol{v}_2^{\rm in} \rangle$ and $\langle p_1^{\rm in} \boldsymbol{v}_1^{\rm in} \rangle$ are negligibly small for a standing wave, we find the following equations for $\langle \boldsymbol{v}_2^{\rm sc} \rangle$ and $\langle p_2^{\rm sc} \rangle$ to leading order,

$$\nabla \cdot \left\langle \boldsymbol{v}_{2}^{\text{sc}} \right\rangle = -\frac{1}{\rho_{0}^{\infty} c_{0}^{\infty 2}} \nabla \cdot \left\langle p_{1} \boldsymbol{v}_{1} \right\rangle_{\text{nii}}, \tag{44a}$$

$$\nu_{0}^{\infty} \nabla^{2} \left\langle \boldsymbol{v}_{2}^{\text{sc}} \right\rangle + \left(\nu_{0}^{\text{bo}} - \frac{2}{3} \nu_{0}^{\infty}\right) \nabla \left(\nabla \cdot \left\langle \boldsymbol{v}_{2}^{\text{sc}} \right\rangle\right) \mathbf{I} - \frac{1}{\rho_{0}^{\infty}} \nabla \left\langle p_{2}^{\text{sc}} \right\rangle \mathbf{I}$$

$$= -\nabla \cdot \left\langle \nu_{1} \left[\nabla \boldsymbol{v}_{1} + \left(\nabla \boldsymbol{v}_{1} \right)^{\mathsf{T}} \right] + \left[\nu_{1}^{\text{b}} - \frac{2}{3} \nu_{1} \right] (\nabla \cdot \boldsymbol{v}_{1}) \mathbf{I} \right\rangle_{\text{nii}}$$

$$+ \nabla \cdot \left\langle \boldsymbol{v}_{1} \boldsymbol{v}_{1} \right\rangle_{\text{nii}} + a_{\rho} \Delta T_{0} \nabla \cdot \left\langle \boldsymbol{v}_{1}^{\text{in}} \boldsymbol{v}_{1}^{\text{in}} \right\rangle, \tag{44b}$$

where the index 'nii' (stands for 'no incident-incident') indicates that terms with products of two first-order incident fields are discarded. In Eq. (44) we have introduced

the kinematic viscosities to zeroth and first order,

$$\nu_0^{\infty} = \frac{\eta_0^{\infty}}{\rho_0^{\infty}}, \qquad \nu_0^{\text{b}\infty} = \frac{\eta_0^{\text{b}\infty}}{\rho_0^{\infty}},$$
 (45a)

$$\nu_1 = \frac{\eta_1}{\rho_0^{\infty}} \approx -B_c^{\infty} \frac{\nu_0^{\infty}}{\rho_0^{\infty} c_0^{\infty 2}} p_1, \tag{45b}$$

$$\nu_1^{\rm b} = \frac{\eta_1^{\rm b}}{\rho_0^{\infty}} \approx -B_c^{\rm b\infty} \frac{\nu_0^{\infty}}{\rho_0^{\infty} c_0^{\infty 2}} p_1.$$
 (45c)

To facilitate the computation of F^{rad} , we note that the incident terms, which make no reference to the particle heating or scattering, cannot contribute to the radiation force, and therefore we obtain the useful expression

$$\oint_{\partial\Omega_{0}} \left\langle \eta_{0}^{\infty} \left[\boldsymbol{\nabla} \boldsymbol{v}_{2}^{\text{in}} + \left(\boldsymbol{\nabla} \boldsymbol{v}_{2}^{\text{in}} \right)^{\mathsf{T}} \right] + \left(\eta_{0}^{\text{boo}} - \frac{2}{3} \eta_{0}^{\infty} \right) \left(\boldsymbol{\nabla} \cdot \boldsymbol{v}_{2}^{\text{in}} \right) \mathbf{I} \right. \\
- p_{2}^{\text{in}} \mathbf{I} + \eta_{1}^{\text{in}} \left[\boldsymbol{\nabla} \boldsymbol{v}_{1}^{\text{in}} + \left(\boldsymbol{\nabla} \boldsymbol{v}_{1}^{\text{in}} \right)^{\mathsf{T}} \right] + \left(\eta_{1}^{\text{b,in}} - \frac{2}{3} \eta_{1}^{\text{in}} \right) \left(\boldsymbol{\nabla} \cdot \boldsymbol{v}_{1}^{\text{in}} \right) \mathbf{I} \\
- \rho_{0}^{\infty} \boldsymbol{v}_{1}^{\text{in}} \boldsymbol{v}_{1}^{\text{in}} \right\rangle \cdot \boldsymbol{n} \, \mathrm{d}S = 0. \tag{46}$$

Then, by subtracting Eq. (46) from Eq. (3), we find,

$$\mathbf{F}^{\mathrm{rad}} = \rho_0^{\infty} \oint_{\partial \Omega_0} \left\{ \left\langle \nu_0^{\mathrm{sc}} \left[\nabla \mathbf{v}_2^{\mathrm{sc}} + \left(\nabla \mathbf{v}_2^{\mathrm{sc}} \right)^{\mathsf{T}} \right] + \left(\nu_0^{\mathrm{b\infty}} - \frac{2}{3} \nu_0^{\infty} \right) \left(\nabla \cdot \mathbf{v}_2^{\mathrm{sc}} \right) \mathbf{I} - \frac{1}{\rho_0^{\infty}} p_2^{\mathrm{sc}} \mathbf{I} \right\rangle \right. \\
\left. + \left\langle \nu_1 \left[\nabla \mathbf{v}_1 + \left(\nabla \mathbf{v}_1 \right)^{\mathsf{T}} \right] + \left(\nu_1^{\mathrm{b}} - \frac{2}{3} \nu_1 \right) \left(\nabla \cdot \mathbf{v}_1 \right) \mathbf{I} - \mathbf{v}_1 \mathbf{v}_1 \right\rangle_{\mathrm{nii}} \\
\left. - a_{\rho} \Delta T_0 \left\langle \mathbf{v}_1^{\mathrm{in}} \mathbf{v}_1^{\mathrm{in}} \right\rangle \right\} \cdot \mathbf{n} \, \mathrm{d}S = 0. \tag{47}$$

The set of equations (44) and (47) determines $\boldsymbol{F}^{\mathrm{rad}}$ similarly to Eqs. (17) and (82) in Ref. [12] (setting $\langle \boldsymbol{v}_{2}^{\text{in}} \rangle = 0$), but differing by the appearance here of the additional terms containing $\langle v_1^{\text{in}} v_1^{\text{in}} \rangle$. However, the solution method remains unchanged, as these new terms are included using the same Helmholtz decomposition and the same partial-wave expansion as for the other terms containing products of first-order fields. From this point, $\langle v_2^{\text{sc}} \rangle$, $\langle p_2^{\text{sc}} \rangle$, and $\boldsymbol{F}^{\text{rad}}$ are thus computed using the same technique as detailed in Ref. [12], Sections IV A, IV B, V A, and Appendix D, and therefore it suffices here simply to summarize the result for $m{F}^{
m rad}$. Since $raket{v_2^{
m in}}$ is neglected here, $m{F}^{
m rad}$ only contains the component consisting of time-averaged first-order products, denoted $\mathbf{F}_{11}^{\mathrm{rad}}$ in Ref. [12] Eqs. (84) and (87), and not the drag-force component, denoted $\textbf{\textit{F}}_{2,\text{in}}^{\text{rad}}$ [12],

$$F^{\text{rad}} = -e_{z}3\pi\rho_{0}^{\infty} \left\{ -\frac{a^{2}\nu_{0}^{\infty}}{\rho_{0}^{\infty}c_{0}^{\infty 2}} \int_{1}^{\infty} d\xi \int_{0}^{\pi} d\theta \cos\theta \sin\theta \nabla \cdot \frac{1}{2} \operatorname{Re} \left[p_{1}\boldsymbol{v}_{1} \right]_{\text{nii}} \right.$$

$$\left. + a^{2} \int_{1}^{\infty} d\xi \int_{0}^{\pi} d\theta \sin\theta \left(1 - \xi^{-2} \right) \frac{1}{2} \operatorname{Re} \left[\boldsymbol{e}_{r} \cdot \left(\boldsymbol{a}_{\rho} \Delta T_{0} \boldsymbol{v}_{1}^{\text{in}} \boldsymbol{v}_{1}^{\text{in}*} \right) \cdot \boldsymbol{e}_{z} + \frac{1}{2} a \xi \left\{ \boldsymbol{a}_{\rho} \Delta T_{0} \nabla \cdot \left(\boldsymbol{v}_{1}^{\text{in}} \boldsymbol{v}_{1}^{\text{in}*} \right) \right\} \cdot \boldsymbol{e}_{\theta} \sin\theta \right.$$

$$\left. + \boldsymbol{e}_{r} \cdot \left(\boldsymbol{v}_{1} \boldsymbol{v}_{1}^{*} - \nu_{1} \left[\nabla \boldsymbol{v}_{1} + \left(\nabla \boldsymbol{v}_{1} \right)^{\mathsf{T}} \right]^{*} - \left[\nu_{1}^{\mathsf{b}} - \frac{2}{3} \nu_{1} \right] (\nabla \cdot \boldsymbol{v}_{1}^{*}) \mathbf{I} \right)_{\text{nii}} \cdot \boldsymbol{e}_{z} \right.$$

$$\left. + \frac{1}{2} a \xi \left\{ \nabla \cdot \left(\boldsymbol{v}_{1} \boldsymbol{v}_{1}^{*} - \nu_{1} \left[\nabla \boldsymbol{v}_{1} + \left(\nabla \boldsymbol{v}_{1} \right)^{\mathsf{T}} \right]^{*} - \left[\nu_{1}^{\mathsf{b}} - \frac{2}{3} \nu_{1} \right] (\nabla \cdot \boldsymbol{v}_{1}^{*}) \mathbf{I} \right)_{\text{nii}} \right\} \cdot \boldsymbol{e}_{\theta} \sin\theta \right]$$

$$\left. + \int_{0}^{\pi} d\theta \frac{\sin\theta}{2} \operatorname{Re} \left[\frac{a^{3}}{x_{s}^{2}} \left(v_{1r} \partial_{r} v_{1r}^{*} + \frac{1}{r} v_{1\theta} \partial_{\theta} v_{1r}^{*} - \frac{1}{r} v_{1\theta} v_{1\theta}^{*} \right) \cos\theta - \frac{a^{3}}{x_{s}^{2}} \left(v_{1r} \partial_{r} v_{1\theta}^{*} + \frac{1}{r} v_{1\theta} \partial_{\theta} v_{1\theta}^{*} - \frac{1}{r} v_{1r} v_{1\theta}^{*} \right) \sin\theta \right]_{\hat{r}=1}^{*} \right\}.$$

We emphasize two differences between this expression for $\boldsymbol{F}^{\mathrm{rad}}$ and expression (87) in Ref. [12] for $\boldsymbol{F}_{11}^{\mathrm{rad}}$. First, two extra terms containing $a_{\rho}\Delta T_{0}\boldsymbol{v}_{1}^{\mathrm{in}}\boldsymbol{v}_{1}^{\mathrm{in}}$ enter in the second integral of Eq. (48). Second, the first-order fields here are different due to the inclusion of a spatially varying T_{0} through the integrals $I_{n}^{(\pm)}(\hat{r},t)$ and their \hat{r} -derivatives, and due to the assumption of an adiabatic acoustic wave which was not enforced in Ref. [12]. Because of the latter, the final result here does not contain any of the combinations of thermal scattering coefficients $\alpha_{t,n}$ that appear in $\boldsymbol{F}_{11}^{\mathrm{rad}}$ of Ref. [12]. The mathematical structure of $\boldsymbol{F}^{\mathrm{rad}}$ is a sum over quadratic terms of scattering coefficients,

$$\begin{split} \boldsymbol{F}^{\mathrm{rad}} &= -\boldsymbol{e}_z 3\pi \rho_0^{\infty} \sum_{n=0}^{\infty} \frac{n+1}{(2n+1)(2n+3)} \operatorname{Re}(A_n A_{n+1}^* D_n), \\ & \text{with } D_n = D_n^0 + D_n^{\Delta T_0}, \\ D_n^i &= S_{00,n}^i + S_{0c,n}^i \alpha_{c,n+1}^{\mathrm{sc},0} + S_{0s,n}^i \alpha_{s,n+1}^{\mathrm{sc}*} + S_{c0,n}^i \alpha_{c,n}^{\mathrm{sc},0} \\ &+ S_{cc,n}^i \alpha_{c,n}^{\mathrm{sc},0} \alpha_{c,n+1}^{\mathrm{sc},0*} + S_{cs,n}^i \alpha_{c,n}^{\mathrm{sc},0} \alpha_{s,n+1}^{\mathrm{sc}*} + S_{s0,n}^i \alpha_{s,n}^{\mathrm{sc}} \\ &+ S_{sc,n}^i \alpha_{s,n}^{\mathrm{sc}} \alpha_{c,n+1}^{\mathrm{sc},0*} + S_{ss,n}^i \alpha_{s,n}^{\mathrm{sc}} \alpha_{s,n+1}^{\mathrm{sc}*}, \quad i = 0, \Delta T_0. \end{split}$$

Here, we have defined the force coefficients D_n and the second-order coefficients $S^i_{kl,n},\ i=0,\Delta T_0$. The force coefficients have been split into the two components D^0_n and $D^{\Delta T_0}_n$, where D^0_n are the force coefficients for $\Delta T_0=0$, and $D^{\Delta T_0}_n$ contains terms that depend on ΔT_0 explicitly or implicitly through $I^{(\pm)}_n(\hat{r},t)$. To determine the the second-order coefficients $S^i_{kl,n}$, we insert p_1 from Eqs. (29f), (33a) and (35) and v_1 from Eqs. (29f) and (29g) with the potentials from Eq. (32) and read off the coefficients in front of each combination of the scattering coefficients. To leading order in the small parameter x_0 , only D^0_0 , D^0_1 , and $D^{\Delta T_0}_n$ contribute to $F^{\rm rad}$. Further, the only leading-order contribution to $D^{\Delta T_0}_n$ arise from terms in $S^{\Delta T_0}_{00,n}$ that scale with $x^2_0 a_c \Delta T_0$. To leading order we obtain

$$D_{n}^{\Delta T_{0}}(t) = \int_{1}^{\infty} \left(1 - \frac{1}{\hat{r}^{2}}\right) \left\{-2a_{c}\Delta T_{0}x_{0}^{2}j_{n}(x_{0}\hat{r})j_{n+1}(x_{0}\hat{r})\right\} + \frac{i}{\hat{r}^{2}} \left[I_{n}^{(+)}(\hat{r},t) + I_{n}^{(-)}(\hat{r},t) - I_{n+1}^{(+)}(\hat{r},t) - I_{n+1}^{(-)}(\hat{r},t)\right] \right\} d\hat{r}$$

$$= 2a_{c}x_{0}^{2} \int_{1}^{\infty} \Delta T_{0} \left[x_{0}\left(\hat{r} - \frac{1}{3\hat{r}}\right)\left(j_{n}^{2}(x_{0}\hat{r}) - j_{n+1}^{2}(x_{0}\hat{r})\right) - \left(1 - \frac{1}{\hat{r}^{2}}\right)j_{n}(x_{0}\hat{r})j_{n+1}(x_{0}\hat{r})\right] d\hat{r}, \qquad (50)$$

where Eq. (35b) and integration by parts was used to reach the final expression. All the coefficients $D_n^{\Delta T_0}$ scale with $x_0^2 a_c \Delta T_0$, although they decrease in magnitude with n, and one may need to evaluate many terms in the sum of Eq. (49) to reach convergence. We note that $D_n^{\Delta T_0}$ does not depend on the boundary-layer thickness δ_s , and thus it can cause significant contributions to $\mathbf{F}^{\mathrm{rad}}$, without entering the viscous limit of $\delta_s \gtrsim a$. In Appendix B

we list all the coefficients $S^0_{ik,0}$ and $S^0_{ik,1}$ needed to compute D^0_0 and D^0_1 . The final expression in the long wavelength limit for $\boldsymbol{F}^{\mathrm{rad}}$ on a heated particle in an incident standing pressure wave is,

$$\mathbf{F}^{\text{rad}} = -\mathbf{e}_{z} \, \pi \rho_{0}^{\infty} \, \text{Re} \left(A_{0} A_{1}^{*} D_{0}^{0} + \frac{2}{5} A_{1} A_{2}^{*} D_{1}^{0} \right)$$
(51)

$$- \mathbf{e}_{z} 3 \pi \rho_{0}^{\infty} \sum_{n=0}^{\infty} \frac{n+1}{(2n+1)(2n+3)} \, \text{Re} \left(A_{n} A_{n+1}^{*} D_{n}^{\Delta T_{0}} \right),$$
with D_{0}^{0} and D_{1}^{0} from Eq. (49b),

$$\alpha_{c,n}^{\text{sc},0} \, \text{for } n = 0, 1, 2 \, \text{from Eq. (40)},$$

$$\alpha_{s,n}^{\text{sc}} \, \text{for } n = 1, 2 \, \text{from Eq. (40)},$$

$$S_{ik,n}^{0} \, \text{for } n = 0, 1 \, \text{from Appendix B},$$

$$D_{n}^{\Delta T_{0}} \, \text{from Eq. (50)}, \, \text{and } A_{n} \, \text{from Eq. (42)}.$$

Finally, using Eq. (24) we approximate $D_n^{\Delta T_0}$ in the limit $t \to \infty$ and find the following expressions for ΔT_0 ,

$$\Delta T_0(\hat{r}, \infty) = \frac{1}{\hat{r}} \, \Delta T_0^{\text{surf}}. \tag{52}$$

This result combined with Eq. (50) leads to the following expression in leading order,

$$D_n^{\Delta T_0}(\infty) = \frac{\pi}{(2n+1)(2n+3)} x_0^2 a_c \Delta T_0^{\text{surf}}.$$
 (53)

IV. RESULTS FOR A STANDING PLANE WAVE

Inserting A_n from Eq. (42) in Eq. (51), we obtain $\boldsymbol{F}^{\mathrm{rad}}$ from a standing plane wave on a spherical particle of radius a to leading order $x_0^3 = k_0^3 a^3$ or $x_0^2 a_c \Delta T_0$,

$$\mathbf{F}^{\text{rad}} = 4\pi \Phi_{\text{ac}} a^3 k_0 E_{\text{ac}} \sin(2k_0 d) \, \mathbf{e}_z, \tag{54a}$$

$$E_{\rm ac} = \frac{1}{4} \kappa_{s0}^{\infty} p_a^2, \tag{54b}$$

$$\Phi_{\rm ac}(t) = \Phi_{\rm ac}^0 + \Phi_{\rm ac}^{\Delta T_0}(t), \tag{54c}$$

$$\Phi_{\rm ac}^0 = \frac{3}{2} x_0^{-3} \operatorname{Re} \left(D_0^0 - 2D_1^0 \right),$$
(54d)

$$\Phi_{\rm ac}^{\Delta T_0}(t) = \frac{3}{2} x_0^{-3} \sum_{n=0}^{\infty} (n+1) \operatorname{Re} \left[(-1)^n D_n^{\Delta T_0}(t) \right], \quad (54e)$$

where we have introduced the usual time-averaged acoustic energy density $E_{\rm ac}$ and acoustic contrast factor $\Phi_{\rm ac}$ [1, 2, 9, 10]. The latter is split as $\Phi_{\rm ac} = \Phi_{\rm ac}^0 + \Phi_{\rm ac}^{\Delta T_0}(t)$ into the sum of an ambient-temperature term $\Phi_{\rm ac}^0$ with $\Delta T_0 = 0$ and a term $\Phi_{\rm ac}^{\Delta T_0}(t)$ due to the particle heating $\Delta T_0 > 0$. A main feature is that heating through ΔT_0 may cause a sign reversal of $\Phi_{\rm ac}$, thus possibly reversing the direction of particle focusing from pressure nodes to anti-node, or vice versa. We obtain the asymptotic limit $\Phi_{\rm ac}^{\Delta T_0}(\infty)$ for long times of the acoustic contrast-factor perturbation $\Phi_{\rm ac}^{\Delta T_0}(t)$ by combining Eqs. (53) and (54e),

TABLE I. Power density P_0 and absorbed power \dot{Q} for the nine cases shown in Fig. 2: a polystyrene particle of radius $a=1,\,2,\,{\rm and}\,\,5\,\,{\rm \mu m}$ in water, oil, and ethanol, respectively.

| \overline{a} | Source | Water | Ethanol | Oil | Unit |
|------------------|-----------|-------|---------|-----|------------------|
| $1\mu\mathrm{m}$ | P_0 | 1800 | 500 | 500 | ${ m GWm}^{-3}$ |
| $2\mu m$ | P_0 | 460 | 130 | 120 | ${ m GW~m}^{-3}$ |
| $5\mu m$ | P_0 | 73 | 20 | 20 | ${ m GWm}^{-3}$ |
| 1 μm | \dot{Q} | 7.7 | 2.1 | 2.1 | μW |
| $2\mu m$ | \dot{Q} | 15 | 4.1 | 4.2 | μW |
| $5\mu m$ | \dot{Q} | 38 | 11 | 10 | μW |

TABLE II. Parameters at $T_0^\infty=300$ K for water [18–21], oil [22–24], ethanol [25–27], and polystyrene [10, 28–32] used in the examples in Fig. 2. We list the parameters necessary to compute ΔT_0 from Eq. (24), the scattering coefficients $\alpha_{i,n}$ from Eq. (40), and the second-order coefficients $S_{ik,n}$ found in appendix Appendix B. Note that κ_{s0} can be found from Eqs. (9) and (16) for a fluid and a solid, respectively. Due to lack of data, we set $\left(\frac{\partial \eta}{\partial \rho}\right)_{\rho_0}=0$ for oil and ethanol.

| Para- | Water | Oil | Etha- | Poly- | Unit |
|--|---------------------|--------|--------|---------|--------------------------------|
| meter | | | nol | styrene | |
| $c_0, c_{\mathrm{lo}0}$ | 1502 | 1445 | 1138 | 2407 | ms^{-1} |
| $c_{ m tr0}$ | _ | _ | _ | 1154 | ${ m ms}^{-1}$ |
| $ ho_0$ | 996.6 | 922.6 | 784 | 1050 | ${ m kg}{ m m}^{-3}$ |
| α_{p0} | 0.275 | 0.705 | 1.104 | 0.209 | $10^{-3} \mathrm{K}^{-1}$ |
| c_{p0} | 4181 | 2058.4 | 2445 | 1241 | $J (kg K)^{-1}$ |
| $k_0^{ m th}$ | 0.61 | 0.166 | 0.167 | 0.154 | $W(Km)^{-1}$ |
| $D_0^{ m th}$ | 1.464 | 0.874 | 0.871 | 1.182 | $10^{-7} \mathrm{m^2 s^{-1}}$ |
| γ_0 | 1.012 | 1.15 | 1.19 | 1.04 | _ |
| η_0 | 0.854 | 57.4 | 1.01 | _ | mPas |
| $\eta_0^{ m b}$ | 2.4 | 85.13 | 1.4 | _ | mPas |
| $\frac{1}{n_0} \frac{\partial \eta}{\partial T} \Big _{0}$ | -0.022 | -0.044 | -0.019 | _ | K^{-1} |
| $\frac{1}{\eta_0} \frac{\partial \eta}{\partial T} \Big _0$ $\frac{1}{\eta_0} \frac{\partial \eta}{\partial \rho} \Big _0$ | -2.3×10^{-4} | _ | _ | _ | $\mathrm{m^3~kg^{-1}}$ |
| $a_c, (29h)$ | 1.7 | -2.2 | -3.0 | _ | $10^{-3} \mathrm{K}^{-1}$ |

$$\Phi_{\rm ac}^{\Delta T_0}(\infty) = \frac{3\pi}{8} \frac{a_c \Delta T_0^{\rm surf}}{x_0}.$$
 (55)

The time evolution of the acoustic contrast factor $\Phi_{\rm ac}(t)$ is found numerically by evaluating $D_n^{\Delta T_0}(t)$ in Eq. (50), with $\Delta T_0(t)$ from Eq. (24) for a polystyrene particle of radius $a=1,\ 2,\ {\rm and}\ 5$ µm in the three different liquids (a) water, (b) ethanol, and (c) oil. We have chosen the heat power density $P_0=3\Delta T_0^{\rm surf}k_0^{\rm th}\alpha^{a^{-2}}$ such that the asymptotic surface temperature increase becomes $\Delta T_0^{\rm surf}=1$ K. The values of the power density P_0 and the absorbed power $\dot{Q}=\frac{4\pi}{3}a^3P_0$ are listed in Table I, and the material parameters are given in Table II. The resulting $\Phi_{\rm ac}$ as a function of time is shown in Fig. 2, where we have used the terms $n\leq 15$ in the sum of Eq. (54e) to reach a satisfactory convergence.

For a polystyrene particle in water, we see in Fig. 2(a)

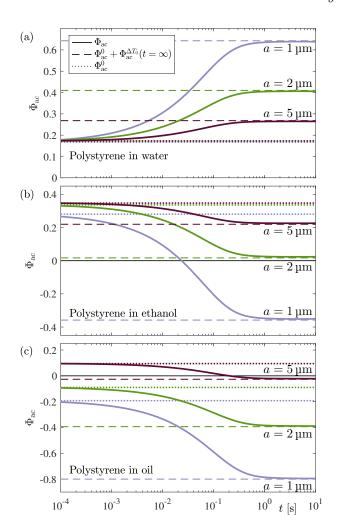


FIG. 2. The acoustic contrast factor $\Phi_{\rm ac}$ at frequency f=1 MHz plotted as function of time t for a polystyrene particle with radius $a=1,\ 2,\ {\rm or}\ 5\,{\rm \mu m}$ heated to $\Delta T_0^{\rm surf}=1$ K in different liquids: (a) water with $t_\lambda^{\rm diff}=2.6$ s, (b) ethanol with $t_\lambda^{\rm diff}=2.5$ s, and (c) oil with $t_\lambda^{\rm diff}=4.0$ s, where $t_\lambda^{\rm diff}=\lambda^2/(6D_0^{\rm th})$ is the heat diffusion time across one wavelength λ .

that for all three particle sizes the initial value of the acoustic contrast factor is nearly the same, $\Phi_{\rm ac}(0)=0.17.$ Even for the largest particle, a=5 µm, the heating induces a 59% increase, $\Phi_{\rm ac}(\infty)=0.27,$ and this effect increases to $\Phi_{\rm ac}(\infty)=0.41$ (141% increase) and 0.64 (276% increase) as the particle radius decreases to a=2 and 1 µm, respectively.

For the two organic liquids ethanol and oil, we see a much stronger effect in Fig. 2(b,c). First, we notice that $\Phi_{\rm ac}(0)$ depends on radius before the onset of the heating, a well-known effect due to the viscous boundary layer, in line with the previous studies of Refs. [4–10, 12]: As radius decreases, $a=5,\ 2,\ {\rm and}\ 1$ µm, we find the decreasing values $\Phi_{\rm ac}(0)=0.35,\ 0.34,\ {\rm and}\ 0.28$ for ethanol, and more pronounced, and even with a sign change, the values $\Phi_{\rm ac}(0)=0.09,\ -0.09,\ {\rm and}\ -0.19$ for oil. Second, we find that the heating of the particle in-

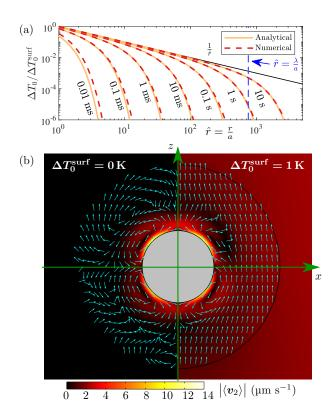


FIG. 3. Results for a polystyrene particle of radius $a=2~\mu m$ in water in a standing plane wave at 1 MHz (wavelength $\lambda=1.5~mm$) and at $T_0^\infty=300~{\rm K}$. (a) The time evolution of the radial temperature deviation $\Delta T_0(\hat{r},t)$ in the fluid for $1<\hat{r}<5000$ computed analytically (orange line) from Eq. (52) and numerically (red dashed line). (b) A unit-vector plot of the direction of the streaming velocity $\langle {\bf v}_2 \rangle$ and a color plot of its amplitude $|\langle {\bf v}_2 \rangle|$ for $\Delta T_0^{\rm surf}=0~{\rm K}$ (left half) and $\Delta T_0^{\rm surf}=1~{\rm K}$ (right half) computed numerically in Comsol Multiphysics.

duces even larger changes in the acoustic contrast factor. For ethanol, heating leads to $\Phi_{\rm ac}(\infty)=0.22,\,0.02,\,{\rm and}\,-0.36$ for decreasing radius $a=5,\,2,\,{\rm and}\,1$ µm, and correspondingly for oil, $\Phi_{\rm ac}(\infty)=-0.03,\,-0.39,\,{\rm and}\,-0.80.$

The observed heat-induced increase $\Phi_{\rm ac}^{\Delta T_0}(t)$ in $\Phi_{\rm ac}$ for water and decrease for ethanol and oil is due to the opposite signs of the thermal sound-speed coefficient a_c , Eq. (29h), of the respective sound speeds c_0 . The effect is so large that we predict a sign reversal in $\boldsymbol{F}^{\rm rad}$ for a polystyrene particle with a=1 µm in ethanol and a=5 µm in oil. Further, $\Phi_{\rm ac}^{\Delta T_0}(t)$ is established by bulk dynamics on a timescale around 1 s, after which it is well approximated by Eq. (55). The physical mechanism causing this change in $\boldsymbol{F}^{\rm rad}$ is the ensuing heating of the bulk fluid by the heated particle that changes the scattered waves defined in Eqs. (25) - (27), which in turn induce the acoustic microstreaming that generates a drag force on the particle, as sketched in Fig. 1.

More details of the physical mechanism causing the heat-induced F^{rad} are illustrated in Fig. 3 for the case of

a 2-µm-radius polystyrene particle suspended in water, subject to a 1-MHz standing, plane, ultrasound pressure wave Eq. (41) of amplitude $p_a=0.1$ MPa and phase shift $k_0d=\frac{1}{3}\pi$, and heated to a surface temperature $\Delta T_0^{\rm surf}=1$ K above the ambient temperature of 300 K. The numerical results were obtained in COMSOL MULTIPHYSICS [33] as described in the Supplemental Material [16].

The time development of the temperature deviation $\Delta T_0(\hat{r},t)$ Eq. (6) in the fluid from ambient temperature, caused by heating of the particle, is plotted in Fig. 3(a). The numerical results show that the analytical long-time-limit expression (52) is a good approximation already after ~ 1 ms. This result constitutes a numerical validation of the model, and it establishes the range of validity of the analytical expression Eq. (52) for $\Delta T_0(\hat{r},t)$. Moreover, it is seen that after ~ 10 s, ΔT_0 has developed into the stationary \hat{r}^{-1} -form in the one-wavelength region $r < \lambda$. This timescale is the same as the heat-diffusion timescale $t_{\lambda}^{\rm diff} = \lambda^2/(6D^{\rm th})$ observed in Fig. 2 for $\Phi_{\rm ac}$ to reach its asymptotic value $\Phi_{\rm ac}^{\Delta T_0}(\infty)$, Eq. (55).

The heat-induced change to the acoustic microstreaming $\langle \boldsymbol{v}_2 \rangle$ around the particle is illustrated in Fig. 3(b). In general at zero heating, $\langle \boldsymbol{v}_2 \rangle$ contains several multipole components, as shown by the unit-vector plot on the left half of the figure ($\Delta T_0^{\rm surf} = 0$ K). Remarkably, the heating of the particle results in a strong enhancement of a unidirectional (dipole) component as shown in the right half of the figure ($\Delta T_0^{\rm surf} = 1$ K). It is this change in morphology of the microstreaming field $\langle \boldsymbol{v}_2 \rangle$ that causes the heating-induced change of the force coefficient $D_n^{\Delta T_0}$ in $\boldsymbol{F}^{\rm rad}$, Eq. (51), and the corresponding change $\Phi_{\rm ac}^{\Delta T_0}$ of the contrast factor, Eq. (54e). The amplitude and direction of the unidirectional component in the microstreaming correlates with the amplitude and sign of $\Phi_{\rm ac}^{\Delta T_0}$, exemplified by the nine examples plotted in Fig. 2.

A key assumption of our analysis is that the heated particle does not execute a significant time-averaged motion, such that the temperature field $\Delta T_0(\mathbf{r},t)$ can develop in the surrounding fluid from a stationary heat source. Since the heat-induced perturbation in \mathbf{F}^{rad} is established on a timescale around 1 s. see Fig. 2, our analysis is primarily relevant for determining the final equilibrium position of the heated particle. The dynamics of slowly-moving particles may be described by the theory, however the description becomes increasingly inaccurate in the transient phase the faster the particle is moving. Regardless of such inaccuracies in the detailed dynamics, our model has a robust prediction regarding whether the particle migrates to a node $(\Phi_{ac} > 0)$ or an antinode (Φ_{ac} < 0) in the pressure field as heating of the particle may change the sign of Φ_{ac} as seen for the 1-um-radius polystyrene particle in ethanol and the 5um-radius polystyrene particle in oil in Fig. 2(b) and (c), respectively. The detailed dynamics only affects the time it takes the particle to reach its temperature-dependent equilibrium position. By combining particle heating with

tuning of the solute by introducing various solvents, other cases of sign reversal in acoustophoresis may be obtained. One example is to add iodixanol to an aqueous solution of particles with an initial positive contrast factor to obtain a negative contrast factor, the so-called medium-tuning technique [34]. Subsequently, a second sign reversal may be obtained by heating the particle.

V. CONCLUSION

We have derived an analytical theory for the acoustic radiation force $F^{\rm rad}$ on a heated spherical solid particle in an incident standing plane wave. The theory assumes that the external or internal heating of the particle is low enough that only small perturbations in the physical parameters of the solid particle and the external fluid occur. Further, effects of thermal convection are assumed negligible. In Section III A we analyze how the temperature increase ΔT_0 diffuses from the heated particle into the surrounding fluid, and we derive the analytical expression (24); in Section IIIB we compute how an incident pressure wave scatters on the slightly heated sphere; and in Section IIIC we derive the main result of our work, the general expression (49a) for $\boldsymbol{F}^{\mathrm{rad}}$ in terms of the force coefficients D_n^i Eq. (49b), as well as the analytical expression (51) for F^{rad} in the longwavelength limit. Furthermore, in relation to Eq. (50), we point out that the heat-induced change $D_n^{\Delta T_0}$ in the force coefficient D_n does not depend on the boundarylayer thickness δ_s , but instead on the scattering induced by the long-range, 1/r-decaying, thermal changes in the bulk acoustic properties of the fluid. Consequently, $\boldsymbol{F}^{\mathrm{rad}}$ can be greatly perturbed by particle heating even for particles of large radius $a \gtrsim \delta_s$ in the long-wavelength limit,

In Section IV, we analyze the changes to $\mathbf{F}^{\mathrm{rad}}$ in an incident standing plane wave, by studying numerically and analytically the changes $\Phi_{\mathrm{ac}}^{\Delta T_0}$ to the acoustic contrast factor due to the temperature increase ΔT_0 caused by the heated particle. We find in Fig. 2 that by heating a polystyrene particle of radius a=1, 2, and 5 µm suspended in water, ethanol, or oil, significant quantitative (up to an order of magnitude) and even qualitative changes (sign reversal) to the acoustic contrast factor Φ_{ac} occur. We point out that the opposite sign in the observed heat-induced change $\Phi_{\mathrm{ac}}^{\Delta T_0}(t)$ of Φ_{ac} for water and for the two organic liquids ethanol and oil is due to the opposite signs of the thermal sound-speed coefficient a_c , see Eq. (29h) and Table II.

The crucial role of microstreaming in causing the observed heat-induced changes in $\boldsymbol{F}^{\mathrm{rad}}$ is illustrated in Fig. 3(b). The analysis shows how a unidirectional component in the microstreaming is strongly enhanced by the heating of the fluid surrounding the heated particle. The drag force resulting from this microstreaming component is a main cause of the resulting changes of the acoustic radiation force $\boldsymbol{F}^{\mathrm{rad}}$.

We have extended the analytical theory of the acoustic radiation force on single spherical solid particle suspended in a homogeneous Newtonian fluid, to take into account heating of the particle. Examples where particle heating may greatly affect the force on the particle are explored. The heat-induced change in the acoustic contrast factor found in this work provides an additional control parameter for acoustofluidic handling of suspended microparticles. We speculate that this control may be obtained by optical methods such as absorbtion of laser-light by dyed particles. We hope that the presented analysis will inspire experimental efforts in the field of microscale acoustofluidics trying to improve particle-sorting, -separation, and -trapping techniques based on our predictions.

Appendix A: Approximate temperature profile around uniformly heated sphere

The solution to the heat diffusion problem described in Section III A can be found in Ref. [17], and adapted to the notation used in this work one has,

$$\Delta T_0'(\hat{r}, t) = \frac{Pa^2}{3k_0^{\text{th}/\infty}} \left[\tilde{k}_0^{\text{th}\infty} + \frac{1}{2} \left(1 - \hat{r}^2 \right) - \frac{6}{\pi \hat{r}} \sqrt{\frac{1}{\tilde{\rho}_0^{\infty} \tilde{c}_{p0}^{\infty} \tilde{k}_0^{\text{th}\infty}}} \int_0^{\infty} \frac{e^{-\xi^2 t/t_d^{\text{th}}}}{\xi^2} \frac{\left[\sin \xi - \xi \cos \xi \right] \sin \left(\xi \hat{r} \right)}{\left[g(\xi) \right]^2 + \frac{1}{\tilde{\rho}_0^{\infty} \tilde{c}_{p0}^{\infty} \tilde{k}_0^{\text{th}\infty}} \xi^2 \sin^2 \xi} \, \mathrm{d}\xi \right], \quad (A1a)$$

$$\Delta T_0(\hat{r}, t) = \frac{P_0 a^2}{3k_0^{\text{th}\infty} \hat{r}} \left[1 - \frac{6}{\pi} \int_0^\infty \frac{e^{-\xi^2 t/t_d^{\text{th}}}}{\xi^3} K(\xi, \hat{r}) \,d\xi \right], \tag{A1b}$$

$$K(\xi, \hat{r}) = \frac{\left[\sin \xi - \xi \cos \xi\right]}{\tilde{k}_0^{\text{th}\infty}} \frac{\sqrt{\frac{1}{\tilde{\rho}_0^{\infty} \tilde{c}_{p0}^{\infty} \tilde{k}_0^{\text{th}\infty}}} \xi \sin \xi \cos \left[\sqrt{\tilde{D}_0^{\text{th}\infty}} \xi \left(\hat{r} - 1\right)\right] - g(\xi) \sin \left[\sqrt{\tilde{D}_0^{\text{th}\infty}} \xi \left(\hat{r} - 1\right)\right]}{\left[g(\xi)\right]^2 + \frac{1}{\tilde{\rho}_0^{\infty} \tilde{c}_{p0}^{\infty} \tilde{k}_0^{\text{th}\infty}} \xi^2 \sin^2 \xi},$$
(A1c)

$$g(\xi) = \left[1 - \left(\tilde{k}_0^{\text{th}\infty}\right)^{-1}\right] \sin \xi - \xi \cos \xi. \tag{A1d}$$

For $t \gtrsim 5 t_{\rm d}^{\rm th}$, the function $\frac{{\rm e}^{-\xi^2 t/t_{\rm d}^{\rm th}}}{\xi^3}$ decays so rapidly that the integral in Eq. (A1b) is well approximated by using the leading order in ξ of $K(\xi,\hat{r})$, $K(\xi,\hat{r}) \approx \frac{\xi^2}{3} \sin\left(\sqrt{\tilde{D}_0^{\rm th\infty}}\xi\hat{r}\right)$, where we have kept in mind that $\xi\hat{r}$ can still be large. Using

$$\frac{6}{\pi} \int_0^\infty \frac{e^{-\xi^2 t/t_d^{\text{th}}}}{3\xi} \sin\left(\sqrt{\tilde{D}_0^{\text{th}\infty}} \xi \hat{r}\right) d\xi = \text{erf}\left(x_D^{\text{th}} \hat{r}\right),\tag{A2}$$

we arrive at the result in Eq. (24).

Appendix B: The second-order coefficients $S_{ik,n}$ for a solid particle in a fluid

The 13 $S_{ik,n}$ coefficients that contribute to D_n^0 to leading order in x_0 are stated: 7 coefficients for n = 0 and 6 for n = 1. For the remaining 16 coefficients in modes n = 0 and n = 1, we only state their order in x_0 here.

$$S_{00,0} = \frac{x_0^3}{3x_s^2}, \qquad S_{00,1} = \frac{x_0^3}{3x_s^2}, \qquad S_{0c,0} = \frac{2\mathrm{i}}{3}, \qquad S_{0c,1} \sim \mathcal{O}(1), \qquad S_{0s,0} = -x_0^2 \frac{2\mathrm{i}(1+B_c^\infty)}{x_s^2} \mathrm{e}^{-x_s}, \qquad S_{0s,1} \sim \mathcal{O}(x_0^3),$$

$$S_{c0,0} = \frac{2\mathrm{i}}{3}, \qquad S_{c0,1} = \frac{2\mathrm{i}}{3}, \qquad S_{cc,0} = \frac{6}{x_s^2 x_0^3}, \qquad S_{cc,1} = \frac{135}{x_s^2 x_0^5},$$

$$S_{cs,0} = \frac{1}{24x_s^4 x_0} \left[\left(-x_s^7 + x_s^6 - 14x_s^5 + 18x_s^4 - 48x_s^3 - 96x_s^2 - 144x_s - 144\right) \mathrm{e}^{-x_s} + E_1(x_s) x_s^6(x_s^2 + 12) \right],$$

$$S_{cs,1} = -\frac{3\mathrm{i}}{4x_s^5 x_0^2} \left[\left(-x_s^7 + x_s^6 - 2x_s^5 + 6x_s^4 + 48x_s^3 + 168x_s^2 + 360x_s + 360\right) \mathrm{e}^{-x_s} + E_1(x_s) x_s^8 \right],$$

$$S_{s0,0} = 0, \qquad S_{s0,1} = x_0^2 \frac{6\mathrm{i}}{5x_s^2} \mathrm{e}^{\mathrm{i}x_s}, \qquad S_{sc,0} = 0,$$

$$S_{sc,1} = \frac{1}{32x_s^4 x_0^3} \left[\left(x_s^{10} + 18x_s^8 \right) E_1(-\mathrm{i}x_s) - \left(x_s^9\mathrm{i} + 16\mathrm{i}x_s^7 + x_s^8 - 12\mathrm{i}x_s^5 + 12x_s^6 - 288\mathrm{i}x_s^3 + 12x_s^4 + 4320\mathrm{i}x_s + 1728x_s^2 - 4320 \right) \mathrm{e}^{\mathrm{i}x_s} \right], \qquad S_{ss,0} = 0,$$

$$S_{ss,1} = -\frac{\mathrm{i}}{2}x_s E_1(x_s - \mathrm{i}x_s) \left(x_s^2 + 9 \right) + \frac{1}{x_s^7} \mathrm{e}^{(-1+\mathrm{i})x_s} \left[\frac{1}{4} (-1+\mathrm{i})x_s^9 + \frac{1}{4}x_s^8 + \frac{1}{2} (-5+4\mathrm{i})x_s^7 + \frac{1}{4} (9+3\mathrm{i})x_s^6 + \frac{1}{4} (9+57\mathrm{i})x_s^5 + \frac{1}{4} (-72+177\mathrm{i})x_s^4 + (-108+72\mathrm{i})x_s^3 - (270+18\mathrm{i})x_s^2 - 270(1+\mathrm{i})x_s - 270\mathrm{i} \right]. \qquad (B1)$$

Here, we have used the exponential integral function defined as $E_1(x) = \int_1^\infty \xi^{-1} e^{-x\xi} d\xi$.

L. V. King, On the acoustic radiation pressure on spheres, Proc. R. Soc. London, Ser. A 147, 212 (1934).

^[2] K. Yosioka and Y. Kawasima, Acoustic radiation pressure on a compressible sphere, Acustica 5, 167 (1955).

^[3] L. P. Gorkov, On the forces acting on a small particle in an acoustical field in an ideal fluid, Sov. Phys.—Dokl. 6, 773 (1962), [Doklady Akademii Nauk SSSR 140, 88 (1961)].

^[4] A. Doinikov, Acoustic radiation pressure on a rigid sphere in a viscous fluid, Proc. R. Soc. A: Math. Phys. Eng. Sci. 447, 447 (1994).

^[5] A. A. Doinikov, Acoustic radiation pressure on a com-

pressible sphere in a viscous fluid, J. Fluid Mech. **267**, 1 (1994).

^[6] A. A. Doinikov, Acoustic radiation force on a spherical particle in a viscous heat-conducting fluid .1. general formula, J. Acoust. Soc. Am. 101, 713 (1997).

^[7] A. A. Doinikov, Acoustic radiation force on a spherical particle in a viscous heat-conducting fluid .2. force on a rigid sphere, J. Acoust. Soc. Am. 101, 722 (1997).

^[8] A. A. Doinikov, Acoustic radiation force on a spherical particle in a viscous heat-conducting fluid. 3. Force on a liquid drop, J. Acoust. Soc. Am. 101, 731 (1997).

^[9] M. Settnes and H. Bruus, Forces acting on a small par-

- ticle in an acoustical field in a viscous fluid, Phys. Rev. E 85, 016327 (2012).
- [10] J. T. Karlsen and H. Bruus, Forces acting on a small particle in an acoustical field in a thermoviscous fluid, Phys. Rev. E 92, 043010 (2015).
- [11] A. A. Doinikov, J. Fankhauser, and J. Dual, Nonlinear dynamics of a solid particle in an acoustically excited viscoelastic fluid. I. Acoustic streaming, Phys. Rev. E 104, 065107 (2021).
- [12] B. G. Winckelmann and H. Bruus, Acoustic radiation force on a spherical thermoviscous particle in a thermoviscous fluid including scattering and microstreaming, Phys. Rev. E 107, 065103 (2023).
- [13] J. H. Joergensen and H. Bruus, Theory of pressure acoustics with thermoviscous boundary layers and streaming in elastic cavities, J. Acoust. Soc. Am. 149, 3599 (2021).
- [14] C. P. Lee and T. G. Wang, The acoustic radiation force on a heated (or cooled) rigid sphere—theory, J. Acoust. Soc. Am. 75, 88 (1984).
- [15] C. P. Lee and T. G. Wang, Acoustic radiation force on a heated sphere including effects of heat transfer and acoustic streaming, J. Acoust. Soc. Am. 83, 1324 (1988).
- [16] See Supplemental Material at https://bruus-lab.dk/files/Winckelmann_Frad_heated_sphere_suppl.zip for details on numerical simulations in COMSOL Multiphysics and comments on temperature dependent material parameters.
- [17] H. Goldenberg and C. J. Tranter, Heat flow in an infinite medium heated by a sphere, Br. J. Appl. Phys. 3, 296 (1952).
- [18] P. B. Muller and H. Bruus, Numerical study of thermoviscous effects in ultrasound-induced acoustic streaming in microchannels, Phys. Rev. E 90, 043016 (2014).
- [19] W. Wagner and A. Pruss, The iapws formulation 1995 for the thermodynamic properties of ordinary water substance for general and scientific use, J. Phys. Chem. Ref. Data 31, 387 (2002).
- [20] M. L. Huber, R. A. Perkins, A. Laesecke, D. G. Friend, J. V. Sengers, M. J. Assael, I. N. Metaxa, E. Vogel, R. Mares, and K. Miyagawa, New international formulation for the viscosity of h2o, J. Phys. Chem. Ref. Data 38, 101 (2009).
- [21] M. L. Huber, R. A. Perkins, D. G. Friend, J. V. Sengers, M. J. Assael, I. N. Metaxa, K. Miyagawa, R. Hellmann, and E. Vogel, New international formulation for the ther-

- mal conductivity of h2o, J. Phys. Chem. Ref. Data **41**, 033102 (2012).
- [22] J. N. Coupland and D. J. McClements, Physical properties of liquid edible oils, J. Am. Oil Chem. Soc. 74, 1559 (1997).
- [23] H. Noureddini, B. Teoh, and L. Davis Clements, Viscosities of vegetable oils and fatty acids, J. Am. Oil Chem. Soc. 69, 1189 (1992).
- [24] S. Ghosh, M. Holmes, and M. Povey, Temperature dependence of bulk viscosity in edible oils using acoustic spectroscopy, J. Food Process. Technol. 8, 1000676 (2017).
- [25] T. Sun, J. Schouten, N. Trappeniers, and S. Biswas, Measurements of the densities of liquid benzene, cyclohexane, methanol, and ethanol as functions of temperature at 0.1 mpa, J. Chem. Thermodyn. 20, 1089 (1988).
- [26] A. S. Dukhin and P. J. Goetz, Bulk viscosity and compressibility measurement using acoustic spectroscopy, J Chem Phys 130, 124519 (2009).
- [27] Pure Component Properties, CHERIC, Chemical Engineering and Materials Research Incformation Center, https://www.cheric.org/research/kdb/hcprop/showprop.php?cmpid=818, accessed 13 May 2023.
- [28] Tables of Acoustic Properties of Materials: Plastics, Onda Corporation, https://www.ondacorp.com/ wp-content/uploads/2020/09/Plastics.pdf, accessed 13 May 2023.
- [29] B. Ellis and R. Smith, eds., Polymers: A Properties Database, 2nd ed. (CRC Press, Boca Raton, FL, 2008).
- [30] E. S. Domalski and E. D. Hearing, Heat Capacities and Entropies of Organic Compounds in the Condensed Phase. Volume III, J. Phys. Chem. Ref. Data 25, 1 (1996).
- [31] S. S. Chang and A. B. Bestul, Heat capacities for atactic polystyrene of narrow molecular weight distribution to 360 K., J. Polym. Sci. A-2 Polym. Phys. 6, 849 (1968).
- [32] D. M. Smith and T. A. Wiggins, Sound speeds and laser induced damage in polystyrene, Appl. Opt. 11, 2680 (1972).
- [33] COMSOL Multiphysics 6.0 (2020), http://www.comsol. com.
- [34] P. Augustsson, J. T. Karlsen, H.-W. Su, H. Bruus, and J. Voldman, Iso-acoustic focusing of cells for sizeinsensitive acousto-mechanical phenotyping, Nat. Commun. 7, 11556 (2016).